Automatic Configuration of Mobile Conveyor Lines

Dohee Lee[1] and Tsz-Chiu Au[1]

***Abstract*— A conveyor belt is an efficient mode of transportation and has been widely utilized to move large quantities of objects in assembly lines, airports, etc. We propose a new conveyor system called *mobile conveyor lines* that can autonomously configure itself to move objects to a given destination. This system is suitable for situations such as disaster areas in which it is difficult to set up a conveyor line manually. We analyze the reachability of a group of mobile conveyor belts and propose an algorithm to check the reachability of a given destination, as well as a method to generate a configuration to guide conveyor belts to connect themselves to reach the destination. Our experimental results show that our algorithms, together with a heuristic that biases the search towards the destination, can quickly generate configurations of conveyor belts for problems that require less than 20 conveyor belts.**

I. INTRODUCTION

Many interesting tasks for mobile robots involve moving objects from one location to another. However, the design of existing mobile robots is not the best for moving a large number of objects as efficiently as possible. For example, the robots in the DARPA Robotics Challenge have limited ability to carry or transport a payload; they would have to make many round trips in order to move all objects out of a disaster zone in a rescue mission. While a robot with a high payload capacity can finish the task in a shorter amount of time, it makes more sense to deploy *conveyor belts* to help robots moving the objects. Conveyor technology, which has been widely used to move materials along manufacturing assembly lines or as a mode of transportation (e.g., escalators), could play a big part in *high throughput* robotic systems.

Today most conveyor belts are used in a stationary position in indoor environments (e.g., assembly lines). Few are designated as *portable* conveyor belts that can be deployed at outdoor locations by human workers. One example is Miniveyors' portable conveyors as shown in Fig. 2. These lightweight conveyor systems allow quick and efficient transportation for a wide variety of materials, making them a good companion for robots in rescue missions. However, these conveyor belts still require humans to setup, making them difficult to be deployed in extreme environments such as disaster areas. We therefore propose to consider conveyor belts as robots and study conveyor belts with its own mobility. We call these robots *mobile conveyor belts*. In this paper, we present a mobile conveyor belt that is an ordinary conveyor belt attached to a mobile platform (see Fig. 1), and study how to make a number of these robots configure themselves autonomously without human intervention.

[1]School of Electrical and Computer Engineering, Ulsan National Institute of Science and Technology, South Korea. {dohee,chiu}@unist.ac.kr

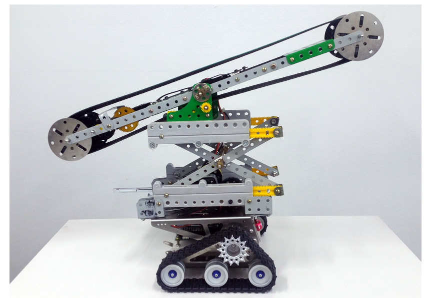

Fig. 1: A mobile conveyor belt.

Fig. 2: A number of Miniveyors forms a conveyor line by stacking their endpoints on top of another's.

One challenge for our mobile conveyor system is how to connect several mobile conveyor belts together to form a *conveyor line* that transfers objects from one location to a given destination. Some destinations simply cannot be reached no matter how the conveyor belts are connected together. Moreover, as the number of conveyor belts increases, the number of possible ways to connect them grow exponentially, causing difficulty in computing the right configurations to form a conveyor line. To resolve these issues,

- we give a *complete* set of equations to describe the set of positions that can be reached by one mobile conveyor belt given its physical constraints;
- we present a probabilistic algorithm to check whether it is possible to use at most N mobile conveyor belts to connect a position to a destination on a flat surface;
- we describe an approach to generate a correct configuration for all conveyor belts if the probabilistic algorithm shows that such configuration exists; and
- we propose a heuristic to increase the chance for the algorithms to find a solution in 3D environments.

This paper is organized as follows. After presenting the related work in Section II, we define our problem in Section III and analyze the reachability of a conveyor belt in Section IV and Section V. Then we give a configuration generation algorithm in Section VI and present the experimental results in Section VII, before we conclude in Section VIII.

II. RELATED WORK

Since robots typically cannot move items in large volumes, we consider incorporating some capabilities of robots into conveyor systems so that the robotic conveyor systems can be used in situations that no other robots can handle. There are few works concerning the configuration of conveyor systems as a whole. Instead, the majority of these works are about the improvement of mechanical design. Li and Li [1] used AMESIM, a hardware modeling software, to evaluate the performance of a conveyor belt and found that the addition of flywheels to motors can greatly improve the performance. Pitcher [2] discussed the loss of strength in three main types of joints between conveyor belts, and found that these joint design cannot perform at their full potential. Donis [3] studied the problem of how to make optimal choice of the locations of the belt weighter while taking the belt stiffness into account. Nuttall [4] studied the design of multiple driven belt conveyors, as well as distributed drive power and tension control, so as to strike a balance between locally applied drive power and the resulting resistances. Bindzar et al. [5] presented a 3D mathematical model of conveyor belt which is used to study its performance when subject to stress loading.

When conveyors are joined, they form a kinematic chain similar to a snake-like robot, which is a type of hyper-redundant manipulation whose configuration problem is mainly about finding collision-free configuration-space paths [14]. Our mobile conveyor line is similar to Job flexible conveyor train, a continuous haulage system for mining applications.[1] These systems are more flexible than mobile conveyor lines we consider here, but their automatic configuration problems are also more complicated.

There are many works on the simulation of conveyor systems. McNearny and Nie [9] and Mankge [10] presented a simulation of underground conveyor system for mining. In particular, Mankge [10] used his simulation to study constraint management of the conveyor haulage systems. Ananth et al. [11] presented a design of a conveyor system that takes belt speed, belt width, motors, pulley, gear box selection, etc., into account. Hou and Meng [12] modeled the dynamic characteristics of a belt conveyor affected by the material of the belt, and observed that the stress wave propagation speed increases with the tensile load. Likewise, Karolewski and Ligocki [13] devised a mathematical model of long belt conveyors that includes phenomena such as the tape's wave behavior and various operating states of the belt.

Energy saving is also a major concern in the design of conveyor systems. Zhang and Xia [6] optimized the energy efficiency of belt conveyors by adjusting operational parameters. Lauhoff [7] critically examined a recommendation about the speed of belt conveyors for energy-saving and found that traditional filling levels is inappropriate. Fonseca et al.[8] proposed an expert system approach to conveyor selection to help making conveyor equipment selection, and showed that it outperformed human experts.

[1] `http://www.joyglobal.com/product-details/flexible-conveyor-train`

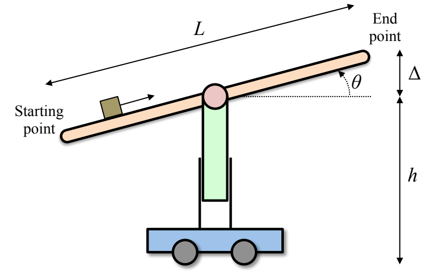

Fig. 3: The design of a mobile conveyor belt.

III. CONFIGURATIONS OF MOBILE CONVEYOR LINES

A conveyor belt is a machine that carries a continuous sequence of objects from one location to another. We attached a conveyor belt to a mobile platform as shown in Fig. 3. The mobile platform connects to the center of the conveyor belt via a strut with adjustable length. At the intersection of the strut and the conveyor belt is a servo motor that controls the slope of the conveyor belt. Let L be the length of the conveyor belt, h be the height of the center of the conveyor belt from the ground, and θ be the *pitch angle* between the conveyor belt and the horizontal plane. Our mobile conveyor belt is height-adjustable and pitch-adjustable, with a minimum height H_{min}, a maximum height H_{max}, and a maximum pitch angle Θ_{max} (i.e., $H_{\mathsf{min}} \leq h \leq H_{\mathsf{max}}$ and $-\Theta_{\mathsf{max}} \leq \theta \leq \Theta_{\mathsf{max}}$). The maximum pitch angle are the same in both clockwise and counterclockwise directions, but the length of a conveyor belt is not adjustable.

A *mobile conveyor line* consists of n mobile conveyor belts linking together at their endpoints to form a chain of conveyor belts. To simplify analysis, we only consider mobile conveyor lines in which all mobile conveyor belts are identical; hence L, H_{min}, H_{max}, and Θ_{max} are the same for all mobile conveyor belts. Let D_{min} and D_{max} be the minimum and maximum vertical distances between the endpoints of two consecutive belts, respectively. If there is a mechanism to physically connect the endpoints of two conveyor belts, we set $D_{\mathsf{min}} = D_{\mathsf{max}} = 0$; otherwise, we can stack one end point of a conveyor belt on top of the end point of another conveyor belt, as shown in Fig .2. In the latter case, D_{max} is the maximum dropping distance the objects can sustain, and $D_{\mathsf{min}} > 0$ because there is a gap between the endpoints of the two conveyor belts.

Let $\tau_1, \tau_2, \ldots, \tau_N$ be N mobile conveyor belts that are put on a flat surface. Let (x_i, y_i) be the coordinate of the center of τ_i, and ϕ_i be the heading of the τ_i. Here the heading of the mobile platform is the same as the heading of the conveyor belt since our conveyor belt cannot rotate relative to the mobile belt. Let h_i and θ_i be the height and the pitch angle of τ_i as depicted in Fig. 3. A *configuration* of τ_i is a 5-tuple $(x_i, y_i, \phi_i, h_i, \theta_i)$. Then the coordinate of the *starting point* of τ_i is $(x_i^{\mathsf{start}}, y_i^{\mathsf{start}}, z_i^{\mathsf{start}}) = (x_i - (L/2)\cos(\theta_i)\cos(\phi_i), y_i - (L/2)\cos(\theta_i)\sin(\phi_i), h_i - (L/2)\sin(\theta_i))$, and the coordinate of the *end point* of τ_i is $(x_i^{\mathsf{end}}, y_i^{\mathsf{end}}, z_i^{\mathsf{end}}) = (x_i + (L/2)\cos(\theta_i)\cos(\phi_i), y_i + (L/2)\cos(\theta_i)\sin(\phi_i), h_i + (L/2)\sin(\theta_i))$.

Objects enter the scene from an *entry point*, which has the coordinate $p^{\text{entry}} = (x^{\text{entry}}, y^{\text{entry}}, z^{\text{entry}})$, where $z^{\text{entry}} \geq 0$. Given N mobile conveyor belts, our goal is to connect n conveyor belts to form a conveyor line that moves objects entering from the entry point to an *exit point* $p^{\text{exit}} = (x^{\text{exit}}, y^{\text{exit}}, z^{\text{exit}})$, where $z^{\text{exit}} \geq 0$ and $0 \leq n \leq N$. In other words, our objective is to compute a set of configurations $\langle (x_i, y_i, \phi_i, h_i, \theta_i) \rangle_{i=1..n}$ for n mobile conveyor belts that satisfies the following constraints:

C1) $x_i^{\text{end}} = x_{i+1}^{\text{start}}$ and $y_i^{\text{end}} = y_{i+1}^{\text{start}}$ for $1 \leq i < n$;

C2) $x_1^{\text{start}} = x^{\text{entry}}$, $y_1^{\text{start}} = y^{\text{entry}}$, $x_n^{\text{end}} = x^{\text{exit}}$, and $y_n^{\text{end}} = y^{\text{exit}}$;

C3) $D_{\text{min}} \leq z_i^{\text{end}} - z_{i+1}^{\text{start}} \leq D_{\text{max}}$ for $1 \leq i < n$;

C4) $D_{\text{min}} \leq z^{\text{entry}} - z_1^{\text{start}} \leq D_{\text{max}}$ and $D_{\text{min}} \leq z_n^{\text{end}} - z^{\text{exit}} \leq D_{\text{max}}$;

C5) $H_{\text{min}} \leq h_i \leq H_{\text{max}}$ and $-\Theta_{\text{max}} \leq \theta_i \leq \Theta_{\text{max}}$ for $1 \leq i \leq n$; and

C6) $z_i^{\text{start}} \geq 0$ and $z_i^{\text{end}} \geq 0$ for $1 \leq i \leq n$.

IV. REACHABILITY ANALYSIS

Due to its physical constraints, a mobile conveyor belt can connect a starting point to a subset of end points in the workspace only. We say these end points are *feasible*. Given a starting point p^{start}, let F be the set of *all* feasible end points. The *reachable set* R of the conveyor belt is the set of points below F such that each point satisfies the dropping distance constraint, i.e., $R = \{(x,y,z') : z - D_{\text{max}} \leq z' \leq z - D_{\text{min}}, (x,y,z) \in F\}$. If a point p is not in R, it means that it is impossible to configure a conveyor belt to move an object from p^{start} to some end point p^{end} and then drop the object to p. As we will see in Section VI, computing the reachable set given a starting point can help to determine if a certain configuration of a conveyor line is feasible. In this section, we will give a complete set of equations to describe the reachable set of one conveyor belt only.

To simplify our discussion, we begin by considering the 2D reachable set on the x-z plane by setting $y = 0$ and $\phi = 0$. We can easily extend this 2D reachable set to 3D by rotating the 2D reachable set along the vertical line passing through the starting point of the conveyor belt—then we get a toroidal region which is the reachable set of the conveyor belt in 3D. Without loss of generality, suppose the starting point of the conveyor belt is fixed at $(0, 0, z^{\text{start}})$. The following equation defines the reachable set in terms of θ:

$$R'(\theta) = \{(x,0,z) : x = L\cos(\theta), z^{\text{start}} + L\sin(\theta) - D_{\text{max}} \leq z \leq z^{\text{start}} + L\sin(\theta) - D_{\text{min}}, z \geq 0\} \tag{1}$$

This reachable set is a vertical line segment whose position and length depend on the value of θ. Let $\theta \in [\theta_a, \theta_b]$ be the valid range of θ such that the conveyor belt satisfies all physical constraints. The reachable set is then

$$R = \bigcup_{\theta_a \leq \theta \leq \theta_b} R'(\theta) \tag{2}$$

The valid range of θ depends on the values of H_{min}, H_{max}, Θ_{max}, L, and z^{start}. Fig. 4 lists the six cases in which the set of the valid range of θ differs. In this figure, $\Delta_{\text{max}} = (L/2)\sin(\Theta_{\text{max}})$ is the maximum vertical distance between the starting point and the center of the belt. In essence, the six cases show how H_{min}, H_{max}, Θ_{max}, and L relate to each other. The range of θ in each case depends on the value of z^{start} as shown in Table I. Some constants in Table I are defined in Table II.

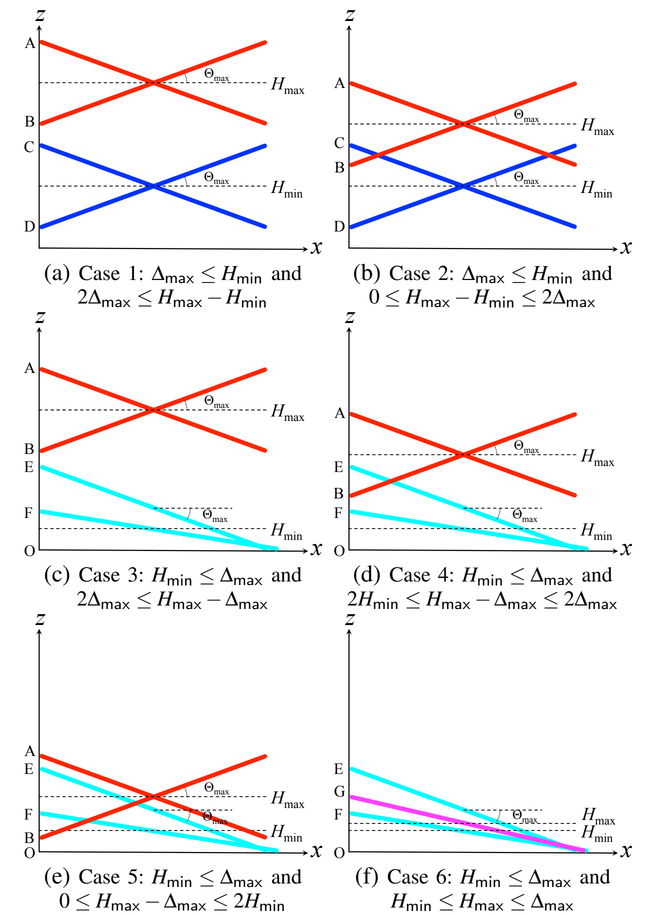

(a) Case 1: $\Delta_{\text{max}} \leq H_{\text{min}}$ and $2\Delta_{\text{max}} \leq H_{\text{max}} - H_{\text{min}}$

(b) Case 2: $\Delta_{\text{max}} \leq H_{\text{min}}$ and $0 \leq H_{\text{max}} - H_{\text{min}} \leq 2\Delta_{\text{max}}$

(c) Case 3: $H_{\text{min}} \leq \Delta_{\text{max}}$ and $2\Delta_{\text{max}} \leq H_{\text{max}} - \Delta_{\text{max}}$

(d) Case 4: $H_{\text{min}} \leq \Delta_{\text{max}}$ and $2H_{\text{min}} \leq H_{\text{max}} - \Delta_{\text{max}} \leq 2\Delta_{\text{max}}$

(e) Case 5: $H_{\text{min}} \leq \Delta_{\text{max}}$ and $0 \leq H_{\text{max}} - \Delta_{\text{max}} \leq 2H_{\text{min}}$

(f) Case 6: $H_{\text{min}} \leq \Delta_{\text{max}}$ and $H_{\text{min}} \leq H_{\text{max}} \leq \Delta_{\text{max}}$

Fig. 4: The six cases in which the set of valid ranges of θ in Table I differs.

To see why the cases in Table I are exhaustive, we need to understand how we identify the six cases in Fig. 4. In Case 1 and Case 2, H_{min} is large enough so that the conveyor belt cannot touch the ground. The red lines represent the conveyor belt when $h = H_{\text{max}}$ at the minimum and maximum pitch angles; Point A and Point B are the starting points of the belt at the minimum and maximum pitch angles, respectively. Likewise, the blue lines represent the conveyor belt when $h = H_{\text{min}}$ at the minimum and maximum pitch angles, whereas Point C and Point D are the corresponding starting points. In Case 1, when z^{start} is between Point A and Point B (i.e., $z_B \leq z^{\text{start}} \leq z_A$ where z_A and z_B are the z-coordinates of A and B, respectively), the maximum θ is limited by H_{max}, while the minimum θ has no limitation except $-\Theta_{\text{max}}$. Hence, the valid range of θ is $[-\Theta_{\text{max}}, \Theta_{\text{upper}}]$, where $\Theta_{\text{upper}} = \arcsin((H_{\text{max}} - z^{\text{start}})/(L/2))$ is the angle at which the conveyor belt is at the maximum height. Similarly, when z^{start} is between Point C and Point D, the minimum θ is limited by H_{min}, while the maximum θ has no limitation except Θ_{max}. Hence, the valid range of θ is $[\Theta_{\text{lower}}, \Theta_{\text{max}}]$, where $\Theta_{\text{lower}} = \arcsin((H_{\text{min}} - z^{\text{start}})/(L/2))$ is the angle at

TABLE I: The range of θ in every case in Fig. 4

Case	Range of z^{start}	Range of θ
1a	$z_B \le z^{\text{start}} \le z_A$	$-\Theta_{\text{max}} \le \theta \le \Theta_{\text{upper}}$
1b	$z_C \le z^{\text{start}} \le z_B$	$-\Theta_{\text{max}} \le \theta \le \Theta_{\text{max}}$
1c	$z_D \le z^{\text{start}} \le z_C$	$\Theta_{\text{lower}} \le \theta \le \Theta_{\text{max}}$
2a	$z_C \le z^{\text{start}} \le z_A$	$-\Theta_{\text{max}} \le \theta \le \Theta_{\text{upper}}$
2b	$z_B \le z^{\text{start}} \le z_C$	$\Theta_{\text{lower}} \le \theta \le \Theta_{\text{upper}}$
2c	$z_D \le z^{\text{start}} \le z_B$	$\Theta_{\text{lower}} \le \theta \le \Theta_{\text{max}}$
3a	$z_B \le z^{\text{start}} \le z_A$	$-\Theta_{\text{max}} \le \theta \le \Theta_{\text{upper}}$
3b	$z_E \le z^{\text{start}} \le z_B$	$-\Theta_{\text{max}} \le \theta \le \Theta_{\text{max}}$
3c	$z_F \le z^{\text{start}} \le z_E$	$\Theta_{\text{floor}} \le \theta \le \Theta_{\text{max}}$
3d	$z_O \le z^{\text{start}} \le z_F$	$\Theta_{\text{lower}} \le \theta \le \Theta_{\text{max}}$
4a	$z_E \le z^{\text{start}} \le z_A$	$-\Theta_{\text{max}} \le \theta \le \Theta_{\text{upper}}$
4b	$z_B \le z^{\text{start}} \le z_E$	$\Theta_{\text{floor}} \le \theta \le \Theta_{\text{upper}}$
4c	$z_F \le z^{\text{start}} \le z_B$	$\Theta_{\text{floor}} \le \theta \le \Theta_{\text{max}}$
4d	$z_O \le z^{\text{start}} \le z_F$	$\Theta_{\text{lower}} \le \theta \le \Theta_{\text{max}}$
5a	$z_E \le z^{\text{start}} \le z_A$	$-\Theta_{\text{max}} \le \theta \le \Theta_{\text{upper}}$
5b	$z_F \le z^{\text{start}} \le z_E$	$\Theta_{\text{floor}} \le \theta \le \Theta_{\text{upper}}$
5c	$z_B \le z^{\text{start}} \le z_F$	$\Theta_{\text{lower}} \le \theta \le \Theta_{\text{upper}}$
5d	$z_O \le z^{\text{start}} \le z_B$	$\Theta_{\text{lower}} \le \theta \le \Theta_{\text{max}}$
6a	$z_F \le z^{\text{start}} \le z_G$	$\Theta_{\text{floor}} \le \theta \le \Theta_{\text{upper}}$
6b	$z_O \le z^{\text{start}} \le z_F$	$\Theta_{\text{lower}} \le \theta \le \Theta_{\text{upper}}$

TABLE II: Definitions of the constants in Fig. 4 and Table I.

$$\Delta_{\text{max}} = (L/2)\sin(\Theta_{\text{max}})$$
$$\Theta_{\text{lower}} = \arcsin((H_{\text{min}} - z^{\text{start}})/(L/2))$$
$$\Theta_{\text{upper}} = \arcsin((H_{\text{max}} - z^{\text{start}})/(L/2))$$
$$\Theta_{\text{floor}} = -\arcsin(z^{\text{start}}/L)$$

which the conveyor belt it at the minimum height. When z^{start} is between Point B and Point C, the pitch angle is not bound by the height, and therefore the valid range of θ is $[-\Theta_{\text{max}},\ \Theta_{\text{max}}]$. z^{start} cannot be larger than z_A or smaller than z_D as the height will exceed the limits. These results are summarized in Cases 1a, 1b, and 1c in Table I.

In Case 2, the range of the height is smaller than $2\Delta_{\text{max}}$, and when z^{start} is between Point B and Point C, the pitch angle is bound by the maximum height and the minimum height at the same time. Apart from this, all other cases are the same as Case 1. These results are summarized in Cases 2a, 2b, and 2c in Table I. Case 2 remains true even when the feasible height range is reduced to zero. Thus there are no other cases to consider when $\Delta_{\text{max}} \le H_{\text{min}}$.

However, when $\Delta_{\text{max}} \ge H_{\text{min}}$, the conveyor belt may touch the ground. Then the minimum pitch angle depends on Point E and Point F at the intersections of the two cyan lines and the z-axis in Fig. 4. Point E is the starting point when the pitch angle is $-\Theta_{\text{max}}$ while the end point touches the ground. Point F is the starting point when the height is H_{min} and the end point touches the ground. When $z^{\text{start}} \ge z_E$, there is no restriction on the lower bound of θ due to the minimum height and the ground. Thus the minimum θ is $-\Theta_{\text{max}}$. When $z_F \le z^{\text{start}} \le z_E$, the lower bound of θ is limited the ground and hence the minimum θ is $\Theta_{\text{floor}} = -\arcsin(z^{\text{start}}/L)$. When $0 \le z^{\text{start}} \le z_F$, the lower bound of θ is once again restricted by the minimum height; thus the minimum θ is Θ_{lower}. All of the above are true in Case 3, Case 4, and Case 5; the only difference in these cases is the location of Point B, causing different combinations of the upper bounds of θ and the lower bounds of θ.

Case 6 is a special case in which H_{max} is small enough so that the belt can always touch the ground even at H_{max}.

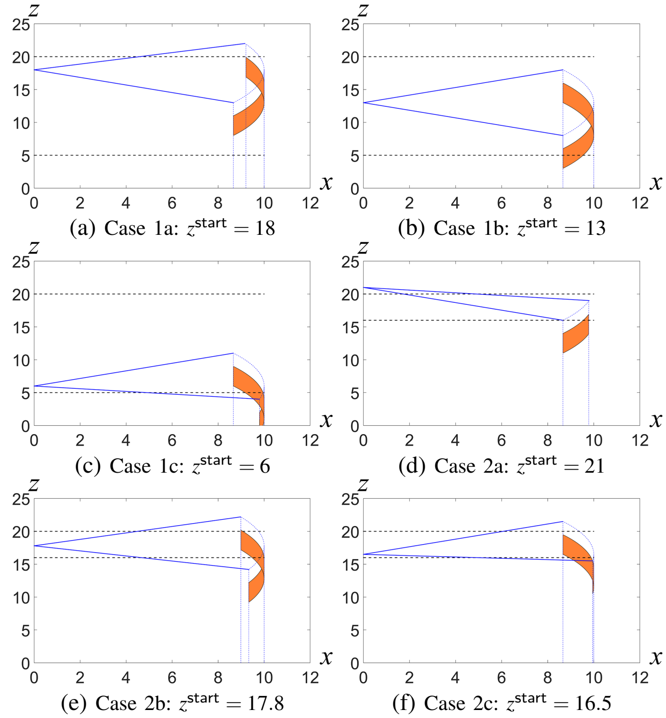

(a) Case 1a: $z^{\text{start}} = 18$ (b) Case 1b: $z^{\text{start}} = 13$ (c) Case 1c: $z^{\text{start}} = 6$ (d) Case 2a: $z^{\text{start}} = 21$ (e) Case 2b: $z^{\text{start}} = 17.8$ (f) Case 2c: $z^{\text{start}} = 16.5$

Fig. 5: Some reachable sets in Case 1 and Case 2. We have $H_{\text{min}} = 5m$ in Case 1 and $H_{\text{min}} = 16m$ in Case 2. Other parameters are $L = 10m$, $H_{\text{max}} = 20m$, $D_{\text{min}} = 2m$, $D_{\text{max}} = 5m$, and $\Theta_{\text{max}} = 30°$.

There is one more special point on the z-axis in this case: Point G is the starting point when $h = H_{\text{max}}$ and the ending point touches the ground (the magenta line in Fig. 4). z^{start} cannot be larger than z_G; otherwise the ending point will go below the ground. The upper bound of θ is always bound by H_{max}, hence $\theta \le \Theta_{\text{upper}}$. The lower bound of θ depends on whether $z^{\text{start}} \ge z_F$.

In Fig. 4 we can see that the line $z = H_{\text{max}}$ gradually approaches the line $z = H_{\text{min}}$ from Case 3 to Case 6. Case 6 is the last case we need to consider because H_{max} cannot be less than H_{min}. Given H_{min}, H_{max}, Θ_{max}, L, and z^{start}, we can find the upper bound and the lower bound of θ from Table I and Fig. 4. Using θ bounds in Eq. 2 yields the reachable set. Fig. 5 shows some examples of the reachable sets (the orange regions) in Case 1 and Case 2. Fig. 5(c) shows the constraint $z \ge 0$ limiting the reachable set.

V. GENERATING CONFIGURATIONS FOR A REACHABLE POINT

Given a point $p = (x, y, z) \in R$ which is reachable from $p^{\text{start}} = (x^{\text{start}}, y^{\text{start}}, z^{\text{start}})$, we want to compute the configuration $(x', y', \phi, h, \theta)$ for a conveyor belt to reach p. In our 2D environments, $y' = y^{\text{start}} = 0$ and $\phi = 0$. Since p^{start} is fixed, we have $x' = x^{\text{start}} + (L/2)\cos(\theta)$ and $h = z^{\text{start}} + (L/2)\sin(\theta)$, both of them depend on θ. To compute θ, consider 1) the vertical line segment $[z + D_{\text{min}},\ z + D_{\text{max}}]$ at x, and 2) the arc of the circle centered at $(x^{\text{start}}, 0, z^{\text{start}})$ with a radius L and a range of angles of the maximum and minimum of θ according to Table I. There are either one

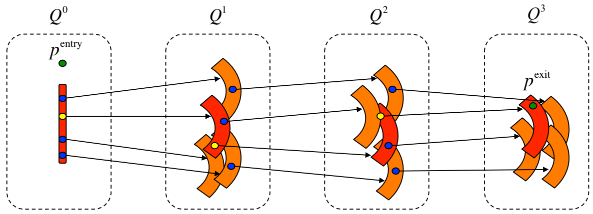

Fig. 6: The search space of the automatic configuration algorithm when $M = 4$ and $N \geq 3$.

or two intersections between the line segment and the arc. These intersections are the end points of the conveyor belt that satisfy the dropping distance constraint to reach $(x,0,z)$. Each intersection can yield a value of θ by $\theta = \arcsin((z'' - z^{\mathsf{start}})/L)$ where z'' is the height of the intersection. Thus there can be two possible configurations to reach $(x,0,z)$.

We can easily extend this calculation to any reachable point (x,y,z) in the 3D toroidal reachable set in 3D environments by transforming p^{start} and (x,y,z) to the x-z plane by a rotation matrix. Then the configuration is $(x^{\mathsf{start}} + (L/2)\cos(\theta), \frac{y+y^{\mathsf{start}}}{2}, \arctan(\frac{y-y^{\mathsf{start}}}{x-x^{\mathsf{start}}}), z^{\mathsf{start}} + (L/2)\sin(\theta), \theta)$ for one or two possible values of θ.

VI. THE AUTOMATIC CONFIGURATION ALGORITHM AND THE OVERLAPPING EFFECT

Based on the reachability analysis in Section IV, we devised Algorithm 1 to generate a configuration for a set of conveyor belts to connect an entry point $p^{\mathsf{entry}} = (x^{\mathsf{entry}}, y^{\mathsf{entry}}, z^{\mathsf{entry}})$ to an exit point $p^{\mathsf{exit}} = (x^{\mathsf{exit}}, y^{\mathsf{exit}}, z^{\mathsf{exit}})$. The algorithm starts from p^{entry} and considers adding conveyor belts one at a time to the conveyor line and randomly computing a *set* of M reachable sets that the newly added conveyor belts may reach, until it finds a reachable set that contains p^{exit} (Line 8). We denote the set of reachable sets after adding the i'th conveyor belt as Q^i. Initially, we set Q^0 to contain only one reachable set, which is the vertical line segment below p^{entry} (Line 2–3). For $i \geq 1$, Q^i is computed by 1) computing the union U_i of the all reachable sets in Q^{i-1} (Line 5), 2) randomly choosing M points in U_i (Line 6), and 3) finding the reachable sets of the chosen points according to Section IV and adding them to Q^i (Line 7). Suppose a reachable set that contains p^{exit} is found after adding n conveyor belts. After that the algorithm searches backward to find the sequence of reachable sets that leads to p^{exit}, as shown in the red regions in Fig. 6. The points $p_0^*, p_1^*, \ldots, p_{n-1}^*$ from which the reachable sets are generated (i.e., the yellow dots in Fig. 6) are the starting points of the n conveyor belts (Line 12–13). Since the algorithm keeps all p_k and R_k^i generated in Line 7, no computation is needed to find p_{i-1}^* in Line 13. Then we can compute a configuration for the entire conveyor line using $p_0^*, p_1^*, \ldots, p_{n-1}^*$ according to Section V (Line 14–16). We can easily verify that this configuration satisfies the constraints C1-C6 in Section III.

Algorithm 1 works in both 2D and 3D environments. In 2D environments, all conveyor belts are aligned on a 2D plane. As shown in Fig. 6, there are many overlaps among reachable sets. This is true in practice because the

Algorithm 1 The automatic configuration algorithm.

1: **procedure** FINDCONFIG($p^{\mathsf{entry}}, p^{\mathsf{exit}}, N, M$)
2: $R_1^0 := \{(x^{\mathsf{entry}}, y^{\mathsf{entry}}, z) : z \in [z^{\mathsf{entry}} - D_{\mathsf{max}}, z^{\mathsf{entry}} - D_{\mathsf{min}}]\}$
3: $Q^0 := \{R_1^0\}$; $n :=$ nil
4: **for** $i := 1$ to N **do**
5: $U_i := \bigcup \{R : R \in Q^{i-1}\}$; $Q^i := \emptyset$
6: Randomly select M points $p_1, \ldots, p_M$ in U_i
7: **for each** p_k, **do** generate R_k^i from p_k; $Q^i := Q^i \cup \{R_k^i\}$
8: **if** there exist k^* such that $p^{\mathsf{exit}} \in R_{k^*}^i$ **then** $n := i$; **break**
9: **if** $n =$ nil **then return** "No solution"
10: $p_n^* := p^{\mathsf{exit}}$
11: **for** $i := n$ **down to** 1 **do**
12: Identify k_i^* and $R_{k_i^*}^i$ such that $p_i^* \in R_{k_i^*}^i \in Q^i$
13: Identify p_{i-1}^* which generated $R_{k_i^*}^i$ in Line 7
14: Compute θ_i for the i'th belt to reach p_i^* from p_{i-1}^*
15: where p_{i-1}^* is the starting point of the belt.
16: Compute $(x_i, y_i, \phi_i, h_i, \theta_i)$ using one of the values of θ_i.
17: **return** $\langle (x_i, y_i, \phi_i, h_i, \theta_i) \rangle_{i=1..n}$

maximum pitch angles and maximum dropping distances are usually quite small, constraining the possible starting points of the next conveyor belt to a small region. We call this observation the *overlapping effect*. Our algorithm exploits this effect by sampling in the union of the set of reachable sets *uniformly* in Line 5–6. As we will demonstrate in our experiment in Section VII, searching with M sampling points simultaneously is better than making M independent searches, each with one sample point. This is because the overlapping region will be less likely to be sampled again due to the overlapping effect.

However, the overlapping effect is less prominent in 3D environments. Due to the freedom in the extra dimension, the algorithm performs poorly if we do not guide the search towards the exit point. Our solution to this problem is to give a higher chance to the sample points that are closer to the exit point. More specifically, in Line 6, we randomly choose $M \times K$ points in U_i for some constant K. Then we assign a weight W_p to each chosen point p, where W_p is a large constant W minus the distance between p and the exit point. After that we randomly select M points out of these chosen points according to their weights, such that points closer to the exit point will have a higher probability to be sampled. As shown in the next section, this heuristic can help finding a solution in 3D environments quickly.

VII. EXPERIMENTAL EVALUATION

We conducted two experiments to evaluate our automatic configuration algorithm in 2D and 3D environments. In the 2D experiment, for each $1 \leq N \leq 20$, we randomly generated 100 *solvable* problems in a 2D environment by choosing the parameters with a uniform probability distribution in the following ranges: $H_{\mathsf{max}} \in [400,\ 600]$, $H_{\mathsf{min}} \in [200,\ 400]$, $L \in [200,\ 400]$, $D_{\mathsf{max}} \in [30,\ 50]$, $D_{\mathsf{min}} \in [5,\ 10]$, $\Theta_{\mathsf{max}} = 30°$, Here, all units except Θ_{max}'s are in centimeter. For each set of parameters, we chose an entry point p^{entry} by setting $x^{\mathsf{entry}} = y^{\mathsf{entry}} = 0$ and choosing $z^{\mathsf{entry}} \in [H_{\mathsf{min}} - (L/2)\sin(\Theta_{\mathsf{max}}),\ H_{\mathsf{max}} + (L/2)\sin(\Theta_{\mathsf{max}})]$. Starting

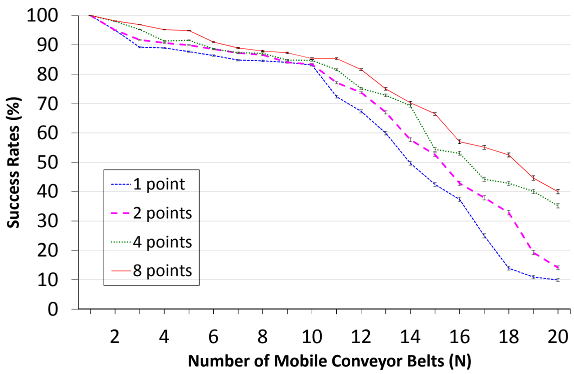

Fig. 7: The success rates in 2D environments.

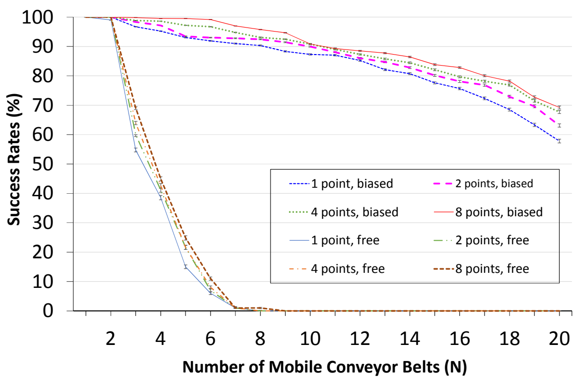

Fig. 8: The success rates in 3D environments.

from p^{entry}, we connected N conveyor belts by randomly choosing a dropping distance $d \in [D_{\mathsf{min}}\, D_{\mathsf{max}}]$ and a pitch angle $\theta \in [-\Theta_{\mathsf{max}},\ \Theta_{\mathsf{max}}]$. We also made sure that the end points of conveyor belts do not go below the ground. After that we chose an exit point p^{exit} within the dropping distance below the end point of the last conveyor belt. Then the pair $(p^{\mathsf{entry}}, p^{\mathsf{exit}})$ is a problem instance that must have a solution (i.e., a configuration exists to connect p^{entry} to p^{exit}).

We ran the algorithm 100 times for each of the following values of M: 1, 2, 4, and 8. For a fair comparison, we gave each run of the algorithm 50 milliseconds and let the algorithm restart if it could not find a solution within the time limit. Then we measured the success rates out of the 100 executions and plotted the graph in Fig. 7. Note that each data point in Fig. 7 is an average of 10000 values, and the error bars are the 95% confidence intervals. As we predicted in Section VI, the algorithm has a higher success rate when M is large. However, in all cases the successful rates decrease gradually as the number of conveyor belts in the problem generation increases.

We repeated the same experiment in a 3D environment. As before, we generated 100 problems for each $N \in [1,\ 20]$. The difference is that we needed to choose ϕ whenever we added a conveyor belt. To make sure that the exit point is sufficiently far away from the entry point, we chose $\phi \in [\phi' - 90°,\ \phi' + 90°]$, where ϕ' is the heading of the last conveyor belt. We ran the algorithm 200 times for 4 different values of M, half used the heuristic proposed in Section VI to bias the search towards the exit point, while the other half searched freely in all directions. We also reduced the time bounding the execution to 20 milliseconds. Fig. 8 shows the results of this experiment. Without using the heuristic to guide the search process, the algorithm cannot find any solution when $N \geq 10$. The overlapping effect is weak in the 3D environment, and thus the differences in success rates for different values of M is not as large as in the 2D experiment.

VIII. CONCLUSIONS AND FUTURE WORK

We proposed to incorporate mobility into conveyor belts and studied how to connect several mobile conveyor belts to form a conveyor line to reach a given destination. Conveyor belts are good at moving a large quantities of objects, and hence can play a larger role in any robotic system in rescue missions or logistic domains. Our key results include a complete set of equations to describe the reachable set of a mobile conveyor belt on a flat surface, which leads to an efficient probabilistic approach for automatic configuration. Our experimental results demonstrated the overlapping effect, which states that the reachable sets are often overlapped. In the future, we would like to study the automatic configuration of mobile conveyor lines subject to limited mobility in rough terrains such as nuclear disaster areas.

ACKNOWLEDGMENT

This work has taken place in the ART Lab at Ulsan National Institute of Science and Technology (UNIST) and was supported by the UNIST Research Fund (1.150012.01).

REFERENCES

[1] G. Li and R. Li, "Belt conveyor modeling and performance simulation based on amesim," in *International Conference on Information and Computing Science*, vol. 4. IEEE, 2009, pp. 304–307.

[2] D. Pitcher, "Joining conveyor belting," *Bulk Handling Today*, pp. 17–20, 2005.

[3] V. Donis, A. Rachkovskii, and V. Sin, "How the conveyor belt length affects belt weigher accuracy," *Measurement Techniques*, vol. 47, no. 2, pp. 163–167, 2004.

[4] A. J. G. Nuttall, "Design aspects of multiple driven belt conveyors," Ph.D. dissertation, TU Delft, Delft University of Technology, 2007.

[5] Peter, Bindzar, G. Anna, and R. Ivica., "3d mathematical model of conveyor belt subjected to a stress loading," *Podzemni Radovi*, vol. 13, pp. 179–188, 2006.

[6] S. Zhang and X. Xia, "Modeling and energy efficiency optimization of belt conveyors," *Applied Energy*, vol. 88, no. 9, pp. 3061–3071, 2011.

[7] H. Lauhoff, "Speed control on belt conveyors-does it really save energy?" *ZKG INTERNATIONAL*, vol. 58, no. 12, pp. 47–+, 2005.

[8] D. J. Fonseca, G. Uppal, and T. J. Greene, "A knowledge-based system for conveyor equipment selection," *Expert Systems with Applications*, vol. 26, no. 4, pp. 615–623, 2004.

[9] R. L. NcNearny and Z. Nie, "Simulation of a conveyor belt network at an underground coal mine," *Mineral Resources Engineering*, vol. 9, no. 3, pp. 343–355, 2000.

[10] K. Mankge, "A simulation approach to constraints management of an underground conveyor system," University of Pretoria, Tech. Rep., 2013.

[11] K. N. S. Ananth, V. Rakesh, and P. K. Visweswarao, "Design and selecting the proper conveyor belt."

[12] Y.-F. Hou and Q.-R. Meng, "Dynamic characteristics of conveyor belts," *Journal of China University of Mining and Technology*, vol. 18, no. 4, pp. 629–633, 2008.

[13] B. Karolewski and P. Ligocki, "Modelling of long belt conveyors," *Eksploatacja i Niezawodność*, vol. 16, 2014.

[14] T. Collins and W.-M. Shen, "Paso: An integrated, scalable pso-based optimization framework for hyper-redundant manipulator path planning and inverse kinematics," Information Sciences Institute, University of Southern Calfornia, Tech. Rep. ISI-TR-697, 2015.